

Short communications

Crystal structure and electrochemical characteristics of non-AB₅ type La–Ni system alloys

Siqi Shi^{a,b,*}, Chuying Ouyang^b, Minsheng Lei^b

^a Department of Physics, Zhejiang Sci-Tech University, Xiasha College Park, Hangzhou 310018, China

^b Department of Physics, Jiangxi Normal University, Nanchang 330027, China

Received 12 July 2006; received in revised form 24 July 2006; accepted 28 September 2006

Available online 15 December 2006

Abstract

The La–Ni system compounds have been prepared by arc-melting method under Ar atmosphere. X-ray diffraction analysis reveals that the as-prepared alloys consist of different phases. The electrochemical properties, including activation, maximum discharge capacity, high rate chargeability (HRC), and high rate dischargeability (HRD) of these alloy electrodes have been studied through the charge–discharge cycle testing at different temperatures and charge (or discharge) currents. Among the La–Ni alloy electrodes studied, LaNi_{2.28} alloy has the most excellent high rate charging performance, and La₂Ni₇ alloy exhibit the highest high rate dischargeability, while La₇Ni₃ alloy is capable of discharging at low temperature. © 2006 Elsevier B.V. All rights reserved.

Keywords: Ni–MH battery; Hydride electrode alloy; High rate chargeability; High rate dischargeability

1. Introduction

Recently, secondary battery with high energy density and long cyclic life is earnestly demanded as a power source for portable appliances and zero emission vehicles. Due to high specific energy, high resistance to overcharging and overdischarging, capability of performing high rate charge/discharge, environmental friendliness, and interchangeability with a nickel–cadmium batter, nickel–metal hydride batteries (Ni–MH) battery has been widely investigated and applied in portable telecommunication equipment, electric tools and electric vehicles [1–3].

AB₅ alloys, where A represents a metal that is capable of reacting exothermically with hydrogen and B represents another kind of metal, are generally employed as the negative electrode material in Ni–MH. Among this type of alloys (AB₅ alloys), LaNi₅ is the first one that has been studied extensively as an electrode material in Ni–MH batteries [4], which is attribute to its easy reaction with hydrogen at normal temperature. However, repeated improvements to increase the capacity have already realized very high utilization of the intrinsic capacity of the LaNi₅ alloy. Therefore, new type alloys with higher energy den-

sity, faster activation, better rate dischargeability, and lower cost are urgently needed to replace the conventional rare earth-based AB₅-type alloys.

Dump et al. [5] pointed out that AB₃, A₂B₇ and AB₅ are closed related according to the following relationships:

$$3(AB_3) = (AB_5) + 2(AB_2)$$

and

$$(A_2B_7) = (AB_5) + (AB_2)$$

From the viewpoint of gas–solid reactions, Oesterreicher et al. [6] studied the hydrides of La–Ni compounds. Their results showed that the hydrogen storage capacity of the La–Ni compounds increase in the order of LaNi₅ < La₂Ni₇ < LaNi₃ < LaNi₂ < LaNi. Based on the reasons mentioned above, we can rationally believe that La₂Ni₇, LaNi₃, LaNi₂, and LaNi alloys are all potential candidates for the electrode material in metal hydride batteries.

Although there are some studies on non-AB₅ type La–Ni system compounds by far, the results are still quite incomplete; moreover, the electrode characteristics of these alloys have rarely been paid to attention [7]. This paper, as a part of research results in our laboratory, the crystal structure and electrochemical characteristics of non-AB₅ type La–Ni alloys (La₂Ni₇, LaNi₃, LaNi_{2.28}, La₂Ni₃, LaNi and La₇Ni₃) were

* Corresponding author. Tel.: +86 571 86843222; fax: +86 571 86843222.
E-mail address: siqishi@yahoo.com (S. Shi).

extensively studied. We wish this would provide useful information on the generalization of the non-AB₅ type La–Ni system metal hydrides.

2. Experimental details

2.1. Alloy preparation, X-ray diffraction

All alloys were prepared by arc-melting the constituent metals or master alloy on a water-cooled copper hearth under argon atmosphere. The purity of the metals, La and Ni, is higher than 99.9 mass%, respectively. The samples were all inverted and remelted 5 times to ensure good homogeneity. Thereafter, these alloys were crushed into fine powders of 200–300 mesh in mortar.

Crystallographic characterization of the hydrogen storage alloys were investigated by X-ray diffraction on Rigaku D/Max 2500PC X-ray diffractometer (Cu K α , monochromator) using JADE5 software [8]. The cell parameters of the alloys were calculated by Cell program [9].

2.2. Electrochemical measurement

The well-mixed alloy powder and carbonyl nickel powder in weight ratio of 1:5 were pressed into the tablets as metal hydride electrode, which had the diameter of 13 mm and thickness of 1.5 mm, and the weight of each electrode was about 0.9 g.

The electrochemical properties were then measured in a standard three electrode cell consisting of a working electrode (metal hydride electrode), a counter-electrode (NiOOH/Ni(OH)₂ electrode), and a reference electrode (Hg/HgO electrode). The electrolyte in the cell was 6 M KOH aqueous solution. Charge and discharge tests were carried out on an automatic galvanostatic system (DC-5). The emphasis of these charge/discharge tests was on the electrochemical capacity and stability of the negative electrode, thus the capacity of the positive electrode plate was designed to be much higher than that of the negative electrode. At 298 K, these experimental cells were firstly charged at 60 mA g⁻¹ for 5 h followed by a rest for 30 min and then were discharged at the same discharge current density to the cut off voltage of -0.60 V versus Hg/HgO.

To evaluate the HRD (in the range of 60–600 mA g⁻¹), the charging current density was kept constant at 60 mA g⁻¹ and the obtained discharge capacity was denoted as C_i . On the other hand, when the HRC (60–600 mA g⁻¹) was investigated, the discharging current density was held at 60 mA g⁻¹ and thus we got the discharge capacity (C_j). HRD (or HRC) are generally defined as the ratio of the discharge capacity C_i (or C_j) at the cut off voltage of -0.6 V to the maximum capacity C_{max} , namely: HRD = $C_i/C_{max} \times 100\%$, HRC = $C_j/C_{max} \times 100\%$, respectively.

3. Results and discussion

3.1. Structure characteristic

The X-ray diffraction profiles of the La₂Ni₇, LaNi₃, LaNi_{2.28}, La₂Ni₃, LaNi and La₇Ni₃ alloys are shown in Fig. 1. The results

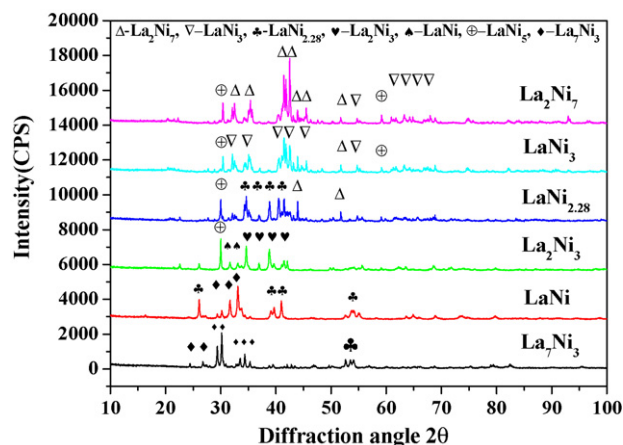


Fig. 1. XRD patterns of La–Ni alloys.

indicate that all the alloys are of multiphase structure. The main phase of the alloys are La₂Ni₇, LaNi₃, LaNi_{2.28}, La₂Ni₃, LaNi, La₇Ni₃, respectively. It is known from La–Ni diagram [10,11] that except LaNi₅ which melt congruently, all the other phases are peritectic. This means that to obtain single phase compounds it is necessary to apply an appropriate annealing treatment generally 2/3 of the melting temperature and below the liquidus during several days. However, we cannot obtain the single phase compounds in our experiment. Fortunately, the main phase of the alloys is La₂Ni₇, LaNi₃, LaNi_{2.28}, La₂Ni₃, LaNi, La₇Ni₃, respectively. The phase composition and lattice parameters are listed in Table 1. It can be seen that LaNi_{2.28} has the largest cell volume and La₇Ni₃ has the smallest density. Further analysis of phase abundance of these alloys is in progress in our laboratory.

3.2. Discharge curves, activation and maximum discharge capacity

Fig. 2 shows the discharge curves (fifth cycle) of the six La–Ni alloy electrodes at 60 mA g⁻¹ and 298 K. As expected, the potential of all the alloy electrodes shift to less nega-

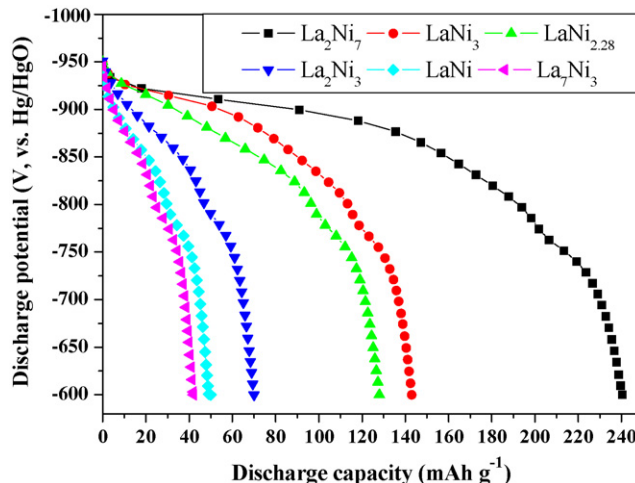


Fig. 2. Discharge curves of the La–Ni alloy electrodes at the discharge current density of 60 mA g⁻¹.

Table 1
Lattice parameter, cell volume and density for the La–Ni alloys

Alloy composition	Lattice parameter			Cell volume (\AA^3)	Density (g cm^{-3})
	a (\AA)	b (\AA)	c (\AA)		
La_7Ni_3	10.149	10.149	6.473	577.44	6.605
LaNi	3.912	10.816	4.399	186.14	7.051
La_2Ni_3	5.114	9.720	7.891	392.26	7.686
$\text{LaNi}_{2.28}$	7.372	7.372	14.555	791.01	8.016
LaNi_3	5.087	5.087	25.128	563.24	8.358
La_2Ni_7	5.067	5.067	24.718	549.69	8.322

tive side due to the oxidation of desorbed hydrogen from the hydride. However, the middle potential (the potential at the 50% depth of discharge) of the alloy electrodes are quite different. They become more and more negative in the order of $\text{La}_7\text{Ni}_3 < \text{LaNi} < \text{La}_2\text{Ni}_3 < \text{LaNi}_{2.28} < \text{LaNi}_3 < \text{La}_2\text{Ni}_7$, i.e. the middle potential shift to more negative side with increasing Ni content in the alloy electrodes. It is known that discharge potential of alloy electrode is associated with the surface activity, the electrolyte concentration, and the internal resistance of the alloy electrode. Moreover, Zhang et al. pointed out that discharge potential is predominated by surface activity at a low discharging rate [12]. The catalysis of Ni element would improve the surface activity of the alloy electrode. So Ni is beneficial to the discharge ability of the alloy electrodes.

When hydrogen storage electrode is first charged, the stored hydrogen in the alloy can be released sparingly during discharge period. The process, that the freshly prepared alloy electrodes are continuously charged and discharged in order to obtain the maximum electrochemical capacity, is called activation. This is important for practical use for Ni–MH battery. Fig. 3 shows the activation profiles of La–Ni alloy electrodes. The results reveal that the activation of all the alloy electrodes only need three cycles, which means that La–Ni alloy electrodes can be easily activated. Taking the discharge capacity into account, we can see that it increases with increasing Ni content in the alloy electrodes. This might be ascribed to the favorable effect of Ni on the middle potential mentioned above. Among the La–Ni alloy electrodes studied, La_2Ni_7 has the highest discharge capac-

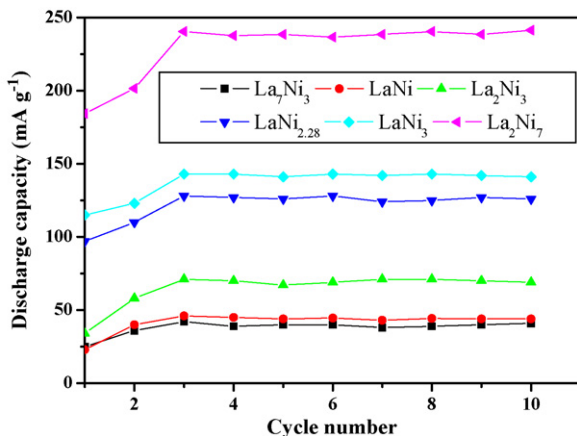


Fig. 3. Specific discharge capacity vs. number of charge/discharge cycles of the La–Ni alloy electrodes.

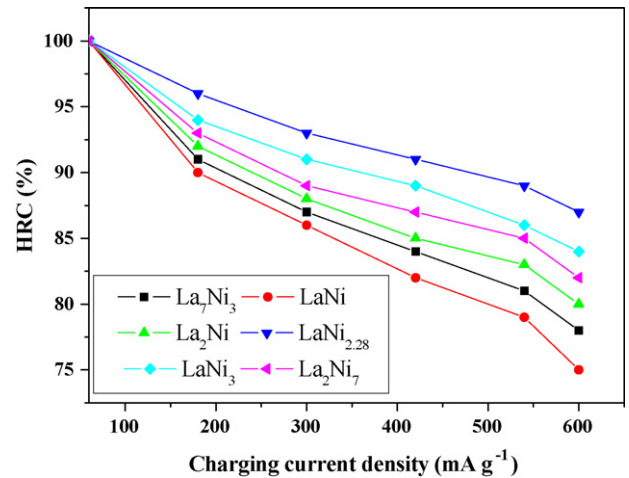


Fig. 4. Effect of charging current density on the high rate chargeability for the La–Ni alloy electrodes (discharging rate: 60 mA g^{-1}).

ity ($240.35 \text{ mAh g}^{-1}$). However, the obtained electrochemical capacities of those La–Ni alloys are far lower than their theoretical capacity. It seems that a further investigation on La–Ni alloys, such as elemental substitution, is needed in order to utilize all the hydrogen stored in the hydride.

3.3. High rate chargeability

High rate chargeability is an important kinetics property for alloy electrode. The dependence of high rate chargeability of the alloy electrodes on the charge current density is demonstrated in Fig. 4. Though all the HRC of the alloy electrodes decreases with increasing charge current density, they still exhibit satisfactory high rate chargeability even at a high charging current density. Taking the charging current density of 600 mA g^{-1} into account, the HRC of all the La–Ni alloy electrodes is higher than 75%. Especially, the $\text{LaNi}_{2.28}$ alloy electrode has a HRC of about 87% even at the charging current density of 600 mA g^{-1} , indicating that $\text{LaNi}_{2.28}$ alloy has the most excellent high rate chargeability among the La–Ni alloy electrodes studied. It is known that there are two main factors that influence the kinetic process of the hydrogen to be stored into or released from the metal hydride electrodes [13,14]. The first is associated with the reactivity of the electrode surface where the charge-transfer process of hydrogen atoms takes place; the second is the diffusion process of hydrogen atoms in the bulk of the hydrogen storage alloy [12]. In this investigation, the Ni content,

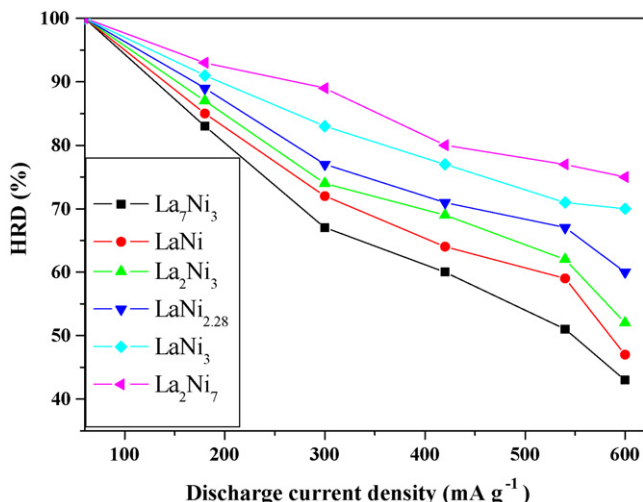


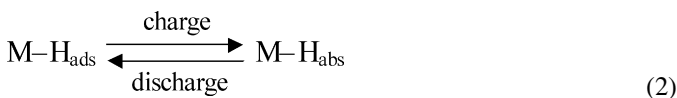
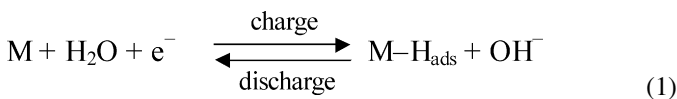
Fig. 5. Dependence of high rate dischargeability on the different discharging rate for the La–Ni alloy electrodes (charging rate: 60 mA g^{-1}).

which is beneficial to surface reaction kinetics, increase in the order of $\text{La}_7\text{Ni}_3 < \text{LaNi} < \text{La}_2\text{Ni}_3 < \text{LaNi}_{2.28} < \text{LaNi}_3 < \text{La}_2\text{Ni}_7$. On the other hand, the cell volume decrease in the order of $\text{LaNi}_{2.28} > \text{La}_7\text{Ni}_3 > \text{LaNi}_3 > \text{La}_2\text{Ni}_7 > \text{La}_2\text{Ni}_3 > \text{LaNi}$. Smaller cell volume is detrimental to the hydrogen diffusion in the bulk of the hydrogen storage alloy and inevitably decreases the high rate chargeability. The joint effect of those two factors result in that $\text{LaNi}_{2.28}$ has the most excellent high rate chargeability among all the alloy electrodes studied.

3.4. High rate dischargeability

It is very important to restrain the decrease of the discharge capacity even at the high discharge current density for practical application of hydride electrode in Ni–MH battery. The dependence of discharge capacity of the La–Ni alloy electrodes on discharge current density is shown in Fig. 5. As expected, the HRD of all the alloy electrodes decays with increasing discharge current density. Nevertheless, the results also indicate that La_2Ni_7 exhibit the highest high rate dischargeability among the alloys investigated.

The electrochemical reactions taking place at the metal hydride electrode in KOH electrolyte during charging and discharging is the following [15]:



where M is the hydrogen storage alloy, M-H_{ads} denotes the adsorbed hydrogen on the surface of the metal hydride and M-H_{abs} refers the absorbed hydrogen in the bulk of the metal hydride. It can be seen from Eqs. (1) and (2), during the discharge process, the hydrogen stored in the bulk of the alloys first diffuses toward the surface in which the adsorbed hydrogen

Table 2

Electrochemical kinetic parameters of La–Ni system alloy electrodes at 298 K

Sample	Exchange current density, I_0 (mA g^{-1})	Hydrogen diffusion coefficient, D ($\times 10^{-10} \text{ cm}^2 \text{ s}^{-1}$)
La_7Ni_3	141.1	9.75
LaNi	153.2	9.79
La_2Ni_3	168.6	9.87
$\text{LaNi}_{2.28}$	181.2	9.93
LaNi_3	201.3	9.82
La_2Ni_7	224.0	9.97

changes to the adsorbed hydrogen, and then the adsorbed hydrogen is oxidized to H_2O . Therefore, the discharge kinetics of the alloy electrodes is controlled not only by the charge-transfer kinetics occurring at the alloy/electrolyte interface, but also by the hydrogen diffusion rate within the bulk of the alloy particles. In general, the charge-transfer kinetics is dominated by the charge-transfer reaction resistance at the alloy surface and the exchange current density I_0 , and the hydrogen diffusion rate is determined by the hydrogen diffusion coefficient D . The I_0 and D obtained using the method described by Iwakura et al. [13] are tabulated in Table 2. It can be seen that the I_0 increases monotonically with increasing Ni content in the alloys, whereas the D remains almost unchanged ($9.75\text{--}9.97 \times 10^{-10} \text{ cm}^2 \text{ s}^{-1}$). Therefore, in the present study, HRD is essentially controlled by the charge-transfer reaction of hydrogen on the surface at a discharge current density of 600 mA h g^{-1} .

3.5. Temperature effect

Alloys used as negative electrode material in Ni–MH battery should be capable of working at wide temperature range. However, the equilibrium pressure of an alloy increase with the increase of working temperature and thus would limit its discharge capacity at high temperature due to decrease of available region in its P – C isotherm under ambient pressure condition. Therefore, it is very important to obtain the factual discharge ability of the alloy electrodes at different temperatures using in situ electrochemical method. Fig. 6

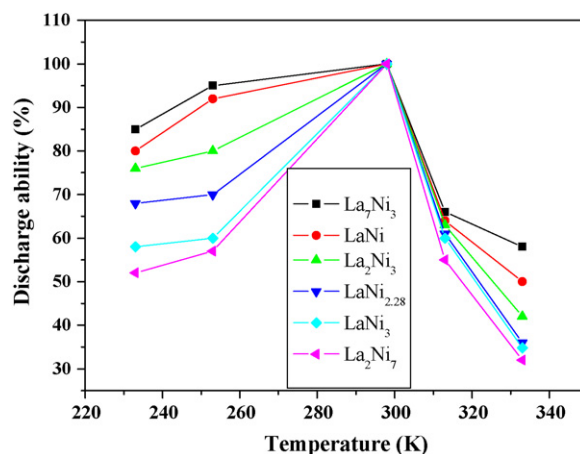


Fig. 6. Discharge ability of La–Ni alloy electrodes as the function of temperature at the discharge current of 60 mA g^{-1} .

shows the discharge abilities of La–Ni alloy electrodes at different temperatures. It can be easily found that the discharge capacities are sensitive to temperature. The electrodes reach their maximum discharge capacities at room temperature (298 K), and then decrease sharply with the decrease and increase of temperature. Especially, at 333 K, all the alloy electrodes can only discharge less than 60% of their maximum capacity, indicating that all the La–Ni alloy electrodes studied have poor high temperature discharge ability. In addition, we can also find that the low temperature discharge ability of the La₇Ni₃ alloy electrode is better than that of the other alloy electrodes. The order of decreasing stability of the hydrides is La₇Ni₃H₂₁ > LaNiH₃ > LaNi₂H₅ > LaNi₃H₅ > LaNi_{3.5}H₄ > LaNi₅H₆ at room temperature [16]. Moreover, it is known that the metal hydride become more and more stable with the decrease of temperature. Decreasing stability of the hydride is beneficial to hydrogen release from the hydride and thereby improves the dischargeability of the alloy electrodes.

4. Conclusion

In this paper, the phase structure and electrochemical properties of La–Ni system alloys have been investigated in detail. It is found that the as-prepared alloys consist of different phases. The electrochemical results show that, among the La–Ni alloy electrodes studied, LaNi_{2.28} alloy has the most excellent high rate charging performance, and La₂Ni₇ exhibit the highest dischargeability. Moreover, La₇Ni₃ is capable of discharging at low temperature. However, the obtained electrochemical capacities of those La–Ni alloy electrodes are far lower than their theoretical capacity. It seems that a further investigation on La–Ni alloy electrodes, such as elemental substitution, is needed in order to utilize all the hydrogen stored in the hydride. If their discharge capacities could be improved, these alloy electrodes

would become promising electrode material in metal hydride battery.

Acknowledgment

This work is supported by National Science Foundation of China (NSFC) under Grant No. 10564002 and 10604023 and Jiangxi Province Science Foundation of China under Grant No. 0512017.

References

- [1] S.R. Ovshinsky, M.A. Fetcenko, J. Ross, *Science* 260 (1993) 176.
- [2] P. Gifford, J. Adams, D. Corrigan, S. Venkatesan, *J. Power Sources* 80 (1999) 157.
- [3] F. Haschka, W. Warthmann, G. Benczru-Urmossy, *J. Power Sources* 72 (1998) 32.
- [4] H. Miyamura, T. Sakai, K. Oguro, A. Kato, H. Ishikawa, *J. Less-Common Met.* 146 (1989) 197.
- [5] B.D. Dump, P.J. Viccaro, G.K. Shenoy, *J. Less-Common Met.* 74 (1980) 75.
- [6] H. Oesterreicher, J. Clinton, H. Bittner, *Mater. Res. Bull.* 2 (1976) 1241.
- [7] J. Chen, N. Krriyama, H.T. Takeshita, H. Tanaka, T. Sakai, M. Haruta, *Electrochim. Solid-State Lett.* 2 (1999) 111.
- [8] Materials Data JADE Realease 5, XRD Pattern Processing, Materials Data Inc. (MDI), 1997.
- [9] Y. Takaki, T. Taniguchand, K. Hori, *J. Ceram. Soc.* 101 (1993) 373.
- [10] J.K. Chang, D.N.S. Shong, W.T. Tsai, *Mater. Chem. Phys.* 83 (2004) 361.
- [11] K.H.J. Buschow, H.H. Van Mal, *J. Less-Common Met.* 29 (1972) 203.
- [12] D. Zhang, J. Tang, K.A. Gschneidner, *J. Less-Common Met.* 169 (1991) 43.
- [13] C. Iwakura, K. Fukuda, H. Senoh, H. Inoue, M. Matsuoka, Y. Yamamoto, *Electrochim. Acta* 43 (1998) 2041.
- [14] J. Han, F. Feng, M. Geng, R. Buxbaum, D.O. Northwood, *J. Power Sources* 80 (1999) 39.
- [15] J.J.G. Willems, *Philips J. Res.* 39 (Suppl. 1) (1984) 1.
- [16] A.J. Maeland, A.F. Andresen, K. Videm, *J. Less-Common Met.* 45 (1976) 347.